www.ietdl.org

Published in IET Power Electronics
Received on 3rd October 2012
Revised on 24th April 2013
Accepted on 12th June 2013
doi: 10.1049/iet-pel.2012.0553

ISSN 1755-4535

Micro-scale inductorless maximum power point tracking DC–DC converter

Alfio Dario Grasso, Salvatore Pennisi

Dipartimento di Ingegneria Elettrica Elettronica e Informatica, University of Catania, Catania, Italy
E-mail: agrasso@dieei.unict.it; dariograsso@ieee.org

Abstract: In this study, the authors propose a simple maximum power point tracking (MPPT) DC–DC converter amenable for micro-scale photovoltaic applications. The solution avoids the use of inductors and exploits a charge pump as a voltage boost element. To take into account the temperature dependence of the MPP voltage, a passive temperature compensation circuit is also included. To validate the idea a prototype was realised with commercial off-the-shelf components. A system efficiency better than 83% for output power above 90 mW is obtained. The results show the viability of the proposed approach which could be further improved through a full custom integrated-circuit design.

1 Introduction

In recent years solar energy harvesting through photovoltaic (PV) conversion has become increasingly significant as a way to improve battery lifetime of portable appliances and stand-alone power systems [1–4]. However, in micro-scale embedded power systems, optimal energy scavenging by exploiting the PV effect poses several challenges, mainly because of the reduced area usable for the cells. Indeed, when the solar cell size scales down to few cm^2, the available power is in the range of few milliwatts [5–11].

In this framework, accurate maximum power point tracking (MPPT) algorithms, which involve complex and power consuming circuits for their implementation, cannot be exploited. Indeed, in those applications where few solar cells are employed, the input power gain is not always higher than the additional power losses that are caused by the MPP tracking operation. Consequently, an MPPT controller for small devices must maximise the net power transfer mainly by minimising the power overhead required by the MPPT implementation. The energy consumption and efficiency of the MPP tracker are, therefore very important design criteria in energy scavengers for solar powered mobile applications [3–9].

The optimisation of the energy harvesting process under varying light irradiance conditions is certainly one of the major design challenges. The output impedance of each PV cell is primarily a function of the irradiance level and temperature. The maximum power point (MPP) is the point on the current–voltage (I–V) curve of the cell that maximises the power output at the given level of light intensity and temperature. In similar way, the amount of power generated by a PV cell (and consequently of a PV module) depends on its operating voltage. It is worth highlighting that a wide variation of the irradiance (200–1000 W/m^2) determines a narrow variation of the MPP voltage, whereas a wide variation of the temperature (10–70°C) determines a more marked variation of the MPP voltage [3, 5, 12]. Hence, the optimal working voltage of the cell depends upon the specific load.

Harvested power can be maximised if the cell and load are impedance matched for every light irradiance and temperature condition. Recently, several MPPT techniques at the array level have been reported in the literature [13–17]. Among them, the perturb-and-observe and the incremental conductance method have drawn more attention. However, they require complex control actions that are often implemented using micro-controllers or DSPs and several current/voltage sensors and analog-to-digital converters [18]. Therefore the major drawback of these methods is the relatively high power consumption required to implement the MPPT circuit, which is not affordable in very low power PV applications. Moreover, these approaches have been effectively used in stand-alone and grid-connected PV solar energy systems and work well under reasonably slow and smoothly changing illumination conditions, mainly caused by weather fluctuations. However, it is not easy to directly apply these approaches into portable PV applications because of low tracking speeds or complex implementations [3, 15].

In this paper, we present a DC–DC converter with embedded MPPT feature that is suitable for applications in the milliwatt power range, like the case of wireless sensor networks supplied by a limited number of PV cells [4–9]. The solution is made up of a charge pump and a voltage comparator plus some passive auxiliary electronics and is amenable for integration with standard CMOS processes. The minimum input voltage is limited by the charge pump capability, whereas the maximum output voltage (and power) is determined by the maximum voltage rating of the adopted technology.

A preliminary prototype using discrete electronic components was fabricated. Namely, the solution exploits the LTC3221 commercial charge pump, the LTC1540 comparator, few resistors and ceramic capacitors, providing a compact and affordable implementation. The MPPT relies on the knowledge of the MPP voltage of the PV cell at nominal temperature, provided by the manufacturer. Finally, a temperature compensation network exploiting a thermistor allows accurate MPPT, over changing PV cell temperature conditions, to be achieved. With the adopted components, that are not optimised for this application, the converter is able to extract the maximum power from an input voltage source ranging from 1.8 to 2.75 V, providing a maximum output power of 330 mW. Better performance could be achieved by a full custom IC design.

2 Proposed circuit

A PV generator, made up of a single or several PV cells (connected in series and/or parallel) is usually connected to the load through a DC–DC power converter circuit, in order to provide the maximum available power to the load. To minimise circuit complexity while optimising energy harvesting, the fractional open circuit voltage (FOCV) method is efficiently used in small-scale PV systems for portable applications [3–7]. This method exploits the nearly linear relationship between the operating voltage at MPP, V_{MPP}, of a typical PV module and its open-circuit voltage, V_{OC}

$$V_{MPP} = K_{FOC} V_{OC} \tag{1}$$

where K_{FOC} is related to the particular PV cell being used, and whose value typically ranges between 0.65 and 0.85. Assuming K_{FOC} to be constant under different irradiance conditions leads to small errors in the V_{MPP} evaluation, but strongly simplifies circuit solutions adopted to implement the MPPT algorithm. This method has proved to be efficient in many solutions reported in the literature [1–7] and has been recently adopted in commercial products [12].

There are two basic types of DC–DC converters, namely inductive and switched-capacitor, SC (also known as charge pumps). Inductive converters (usually, boost or buck) generally show an excellent power conversion efficiency over a wide input voltage operating range, but require bulky inductors in the microhenry range. Even if interleaved techniques can be employed to reduce the value of each inductor, they still would be integrated on silicon with very low efficiency and therefore are left as discrete components [18]. In contrast, the main advantage of SC DC–DC converters is that they require only capacitors and switches which can be fully integrated, thus leading to cost effective solutions [19, 20]. Indeed, standard on-die capacitors can achieve low series resistance and high capacity density can be integrated in current CMOS processes without additional fabrication steps. The main disadvantage of SC DC–DC converters is that they offer high power conversion efficiency only for a limited input voltage range [21]. Although adaptive multi-gain topologies can be profitably exploited in order to overcome this limit [22], this aspect does not constitute a serious problem when PV cells are used as power sources. Indeed, the charge pump can be chosen to maximise efficiency assuming that the input voltage is the MPP one expressed by (1). As a result, in the following we shall adopt the FOCV MPPT method and a charge pump to optimise power harvesting from a micro-scale PV generator. The proposed circuit is based on a SC voltage doubler, whose basic schematic is shown in Fig. 1. The main components of a voltage doubler are four switches, S1–S4, driven by two non-overlapping clock phases, and a flying capacitor C_{fly}. The load is modelled by capacitor C_{load} and resistor R_{load}. During phase Φ_a, switches S1 and S2 are on, charging the flying capacitor to the input voltage. During phase Φ_b switches S1 and S2 are turned off and S3 and S4 are turned on. Consequently, the flying capacitor is placed in series with the input voltage, thus charging the output capacitor to the sum of input voltage and pump capacitor voltage, resulting in a voltage doubling at the output.

The regulation of the input of the charge pump is achieved through on/off control [13, 23]. The simplified schematic of the circuit with the control loop is depicted in Fig. 2. Whenever the input voltage falls below the regulation level (i.e. the cell MPP voltage) the pump is turned off. Once the regulation level is exceeded on the input node, the feedback control signal turns on the pump, allowing power transfer to the output. It is worth noting that during the off state R_{load} is supplied only by C_{load}, which acts as an energy storage element, therefore V_{out} is affected by a voltage ripple that can be reduced by increasing the value of C_{load}. The input voltage of the charge pump with this control loop can be expressed, exploiting the results reported in [23], as

$$V_{in} = V_{out}\left[\frac{1}{2} + 8\frac{R_S}{R_{load}}\left(1 + \frac{t_W}{T}\right)\right] \tag{2}$$

where R_S is the on resistance of each switch, T is the period of the two non-overlapping clock phases and t_W is the blocking

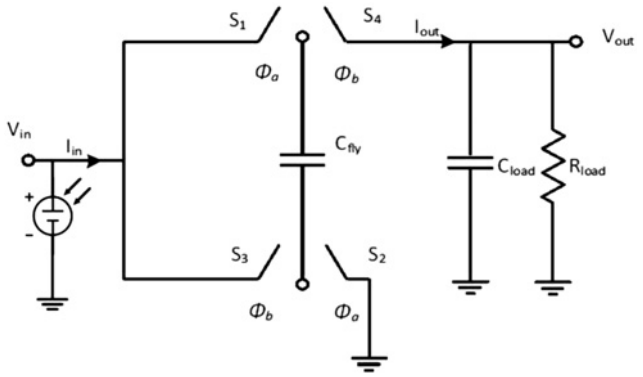

Fig. 1 *Schematic of a voltage doubler*

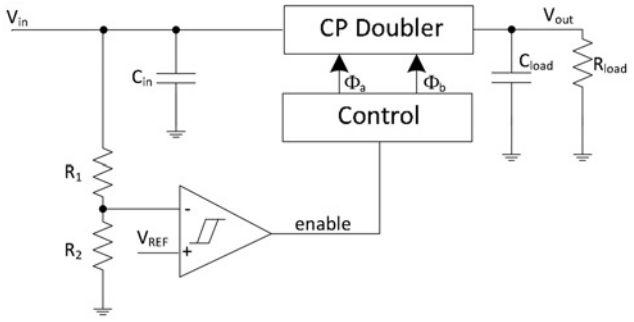

Fig. 2 *Schematic of the control technique*

period, that is, the period of time during which the pump is off. Equation (2) shows that the input voltage, that is the PV cell working voltage, is regulated through t_W, which, in turn, is generated by the comparator and is related to V_{REF} and the voltage divider ratio. Equation (2) also indicates that another way to regulate the input voltage is through the switching frequency of the charge pump during the 'on' state. Nonetheless, this technique requires the implementation of a voltage controlled oscillator which needs additional current consumption. In contrast, the on/off regulation technique constitutes the simplest and most efficient way to obtain a specified input voltage, thus providing MPPT capability. The power conversion efficiency of the system shown in Fig. 2 can be expressed at the steady state by

$$\eta_{conv} = \frac{V_{out}I_{out}}{V_{in}I_{in} + P_{control} + P_{losses}} \tag{3}$$

where V_{in}, I_{in}, V_{out}, I_{out} are the input and output voltage and currents, $P_{control}$ is the power dissipated by the phase generation circuit and the comparator and P_{losses} represents the power loss because of switches and parasitics. Considering that, at the steady state, conservation of energy implies that the input current has to be twice the output current [23], in an ideal unloaded doubling charge pump the efficiency is equal to 1. The efficiency of the system, however, is reduced because of the losses in the switches and equivalent series resistance (ESR) of capacitors. The switch losses can be reduced by adopting optimised topologies and by a proper choice of the switching frequency [19–21, 24]. Owing to the regulation on the input voltage, the output voltage can be assumed almost equal to $2V_{in}$. Therefore when $P_{control}$ and P_{losses} are negligible as compared to the input power, a power transfer efficiency approaching 1 can be achieved using the proposed solution.

In order to test the effectiveness of the proposed solution, the topology shown in Figs. 1 and 2 was implemented by utilising commercial off-the-shelf components. The circuit is shown in Fig. 3. It is based on the charge pump LTC3221 provided by Linear Technologies [25]. In normal operation the output voltage is fed back to the FB pin in order to program the desired output voltage. Our solution is to implement an additional control loop made up of the low-power comparator LTC1540 [26] and a voltage divider connected to the input. This control loop allows the regulation of the working voltage of the PV cell to the MPP value, which is set by [26]

$$V_{MPP,T0} = V_{REF}\left(\frac{R_1//R_{T0}}{R_2} + 1\right) \tag{4}$$

where $V_{MPP,T0}$ is the maximum power point voltage of the specific cell at 25°C, provided by the manufacturer, V_{REF} is the internal reference voltage of the comparator, equal to 1.182 V.

The main drawback of FOCV MPPT method is the dependence of the MPP voltage with the temperature.

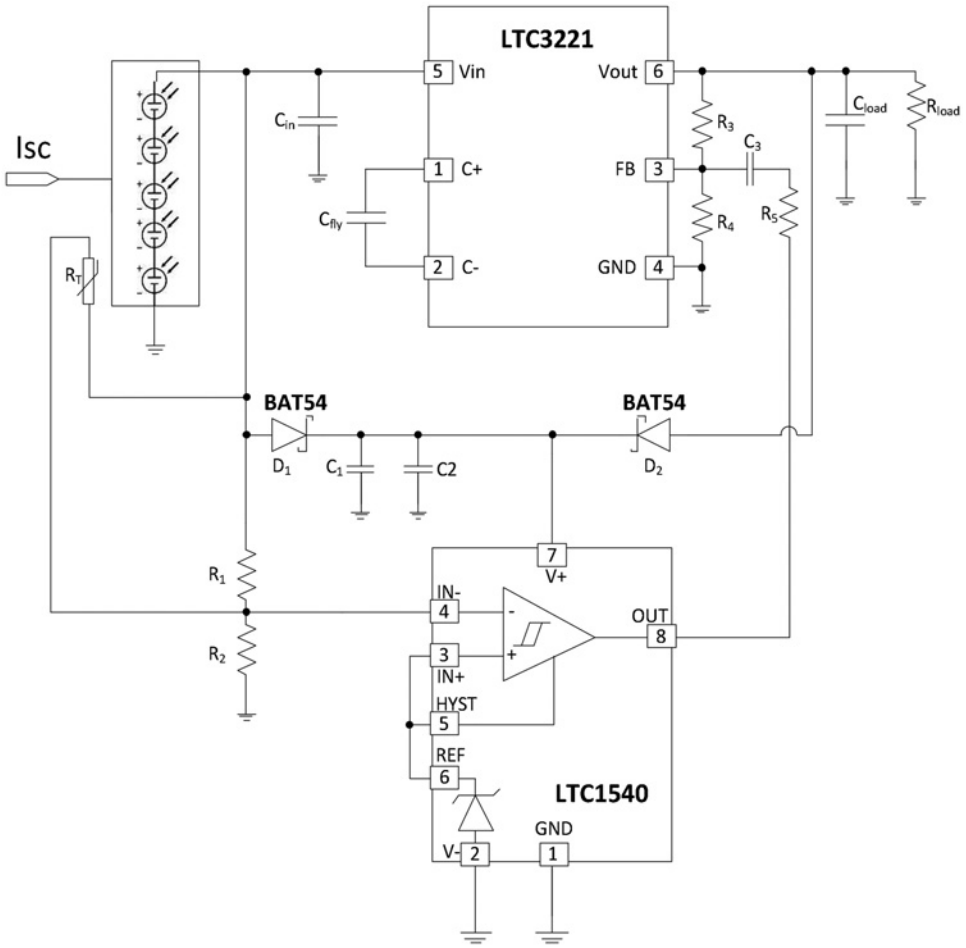

Fig. 3 *Schematic of the proposed solution*

doi: 10.1049/iet-pel.2012.0553

Under the simplified hypothesis that the series resistance R_S is negligible, the relation between V_{OC} and V_{MPP} can be calculated, under open-circuit conditions, as [3]

$$V_{MPP} = \beta_{V_{oc}} V_{OC} - \frac{3}{\gamma} \tag{5}$$

where $\gamma = q/(nKT)$ (q is the electron charge, n is the diode quality factor, K is the Boltzmann constant, T represents the cell temperature) and $\beta_{V_{OC}}$ is the open-circuit voltage temperature coefficient of the specific cell being used. It is apparent that V_{MPP} is a function of temperature through parameters $\beta_{V_{OC}}$ and γ. As the PV cell temperature decreases, V_{MPP} and the available power increase. The peak power point voltage for a PV cell can be approximated at a given temperature as a fixed voltage below V_{OC}, therefore the temperature coefficient for the peak power point is similar to that of V_{OC}. Panel manufacturers usually specify the values of V_{OC}, V_{MPP}, and the temperature coefficient for V_{OC}, at 25°C, making the determination of the temperature coefficient for V_{MPP} straight forward. Therefore V_{MPP} is a function of temperature through

$$V_{MPP}(T) = V_{MPP,T0}\left[1 + \beta_{V_{oc}}(T - T_0)\right] \tag{6}$$

To get rid of the temperature dependence of the MPP voltage, a passive temperature compensation circuit is exploited. The network is shown in Fig. 3. It simply exploits a negative temperature coefficient (NTC) thermistor in parallel with a resistor in order to implement an almost linear negative temperature dependence for the reference voltage at the input of the comparator. The thermistor should be thermally coupled to the PV generator to achieve an accurate temperature tracking. Let us develop a simple model that allows dimensioning the temperature compensation network. The standard formula for NTC thermistor resistance as a function of temperature is given by

$$R_T(T) = R_{T0} e^{(\beta(T_0 - T)/T_0 T)} \tag{7}$$

where R_{T0} is the thermistor nominal resistance at room temperature, β is the thermistor material constant, and T is the actual thermistor temperature. The MPP voltage expression as a function of temperature can be written using (4) and adding R_T, expressed by (7), in parallel to R_2, yielding, after a few algebra

$$\begin{aligned} V_{MPP}(T) &= V_{REF}\left[1 + \frac{R_1 R_{T0}}{R_2 e^{(\beta(T-T_0)/T_0 T)}\left(R_1 + \left(R_{T0}/e^{(\beta(T-T_0)/T_0 T)}\right)\right)}\right] \\ &= V_{REF}\left[1 + \frac{R_1 R_{T0}}{R_2\left(R_{T0} + \left((R_1 e^{\beta/T_0})/(e^{\beta/T})\right)\right)}\right] \end{aligned} \tag{8}$$

The values of the passive network made up of R_1, R_2 and R_T can be found using (4) and equating (6)–(8). Unfortunately, the exponential dependence on T leads to a transcendent equation that can only be solved numerically. Nonetheless, (8) can be well approximated, assuming typical temperature variations, by the linear term of its Taylor series around 25°C, yielding

$$V_{MPP}(T) \simeq V_{MPP,T0} - \beta V_{REF} \frac{R_1^2 R_{T0}(T - T_0)}{T_0^2 R_2 (R_1 + R_{T0})^2} \tag{9}$$

The optimal values of R_1, R_2, R_{T0} and β are found by equating the T coefficients of (6) and (9). A simpler approach relies on assuming $R_2 = R_{T0}$ and equating the coefficient of T between (6) and (9). It leads to

$$\beta = -\frac{T_0^2 R_2 V_{MPP,T0} \beta_{V_{oc}} (R_1 + R_{T0})^2}{R_1^2 R_{T0} V_{REF}} \tag{10}$$

The passive temperature compensation network can be hence designed using the simplified expressions derived above.

We remark that the accuracy of the discussed procedure relies on the knowledge of the MPP voltage at 25°C and the open-circuit voltage temperature coefficient, usually provided by the cell manufacturer. A more accurate temperature compensation technique could be implemented exploiting digital calibration. Nonetheless, the adoption of such a strategy would require additional circuitry, analog-to-digital and digital-to-analog converters, clock generator and so on thereby increasing both the system complexity and power consumption.

In conclusion of this paragraph it should be observed that the use of the thermistor-based temperature compensation network allows a further reduction of the system complexity, compared to the standard FOCV method, since the continuous sampling of the output voltage is no longer required.

3 Simulation results

The proposed circuit in Fig. 3 was preliminarily simulated with SPICE. The PV generator model is obtained by connecting in series five PV cells, each one modelled through the circuit shown in Fig. 4. In this model the irradiance level is emulated through the parameter I_{SC}, (equal to 60 mA) which represents the short circuit current. The simulated V_{MPP} was equal to 2.3 V and the corresponding peak power was equal to 120 mW at 25°C. We set also $R_{load} = 150\ \Omega$ and $C_{load} = 4.7\ \mu F$. Capacitors C_{in}, C_{out} and C_{fly} are equal to 10, 4.7 and 10 µF, respectively. The temperature compensation network was designed following the design equations reported. In particular, assuming $\beta_{V_{OC}} = -8\ mV/°C$, $V_{MPP,T0} = 2.36$ V, $R_1 = R_{T0} = 10\ k\Omega$, (4) and (10) yield $R_1 = 5\ k\Omega$ and $\beta = 2836$. To show graphically how (8) and its approximation (9) fit (6), we plot in Fig. 5, (6), (8) and (9) as a function of temperature. It can be observed that the error introduced by (9) compared to (6) is lower than 10%, in the considered temperature span.

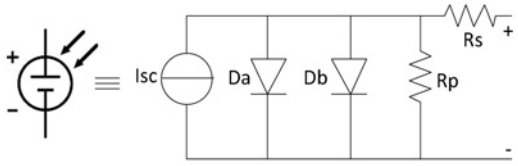

Fig. 4 *Equivalent circuit model of a single PV cell used in simulations*

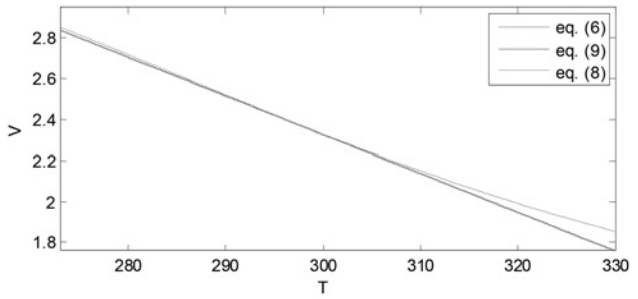

Fig. 5 *Plot of V_{MPP} as given by (6), (8) and (9) against temperature*

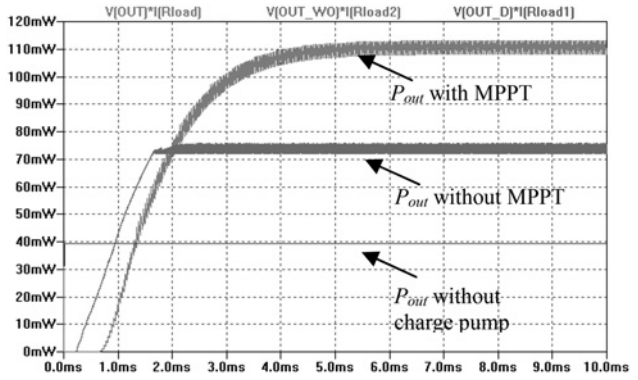

Fig. 6 *Comparison of the power extracted, P_{OUT} ($I_{SC} = 60$ mA, $R_{load} = 150$ Ω)*

Without the control loop the input voltage is above the MPP level causing a power extraction loss, problem that is largely avoided through the proposed circuit. Indeed, as shown in Fig. 6, the power at the output of the proposed circuit is greater than 100 mW, whereas using the same charge pump without the additional control loop, the power decreases to 74 mW and collapses to 40 mW if the PV generator is directly connected to the load. The average simulated power consumption of the additional circuitry used to implement MPPT is equal to 150 µW with a peak value of 435 µW when the output of the comparator switches on.

The circuit was simulated also for different values of the available power from the PV generator (i.e. I_{SC}) and of the load. The efficiency is higher than 90% for output load values greater than 150 Ω, whereas the efficiency reduces for lower values of R_{load} since the charge pump cannot deliver the current necessary to reach the maximum achievable output voltage.

4 Experimental results

In order to further prove the effectiveness of the proposed system, the circuit shown in Fig. 3 was fabricated and tested. Fig. 7 shows the fabricated board whose dimension is 27×40 mm^2. The PV generator adopted is a 44×60 mm^2 thin film cell, showing an MPP voltage equal to 2.36 V at standard test condition (STC) and a corresponding maximum power equal to 120 mW.

The thermistor adopted is Cantherm MF52A103H3100 ($\beta = 3100$ K, $R_{T0} = 10$ kΩ) and was thermally coupled by sealing it to the back of the cell through thermal grease.

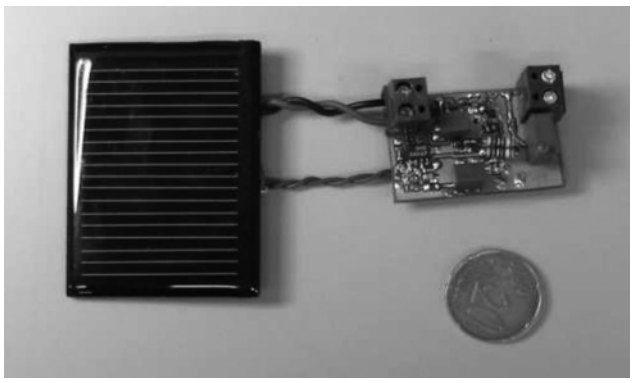

Fig. 7 *Photo of the fabricated printed circuit board supplied by a thin film PV cell*

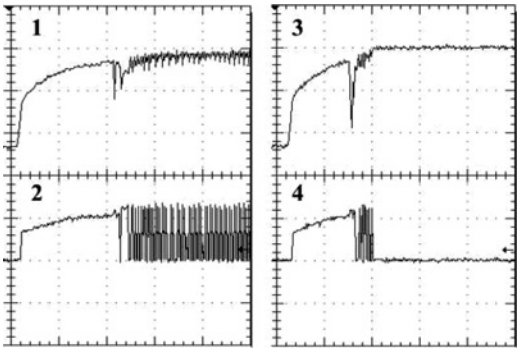

Fig. 8 *Measured start-up transient; 1 and 2: output voltage and comparator output under heavy load; 3 and 4: output voltage and comparator output under light load (xdiv = 1 ms, ydiv = 2 V)*

Inset 1 and 2 in Fig. 8 shows the measured start-up transient of the circuit under heavy output load. The MPPT control loop starts working after about 2 ms. Inset 3 and 4 illustrates the same transient but with lighter output load. Here, the MPPT control loop works only during a shorter period of time needed by the circuit to reach the steady state.

Fig. 9 depicts the measured efficiency of the system against the output load for different values of temperature. Note that the efficiency is obtained as the product of (3) and the tracking efficiency, that is input power over maximum power available from the PV cell. It can be observed that for output loads higher than about 160 Ω the system efficiency is higher than 80%.

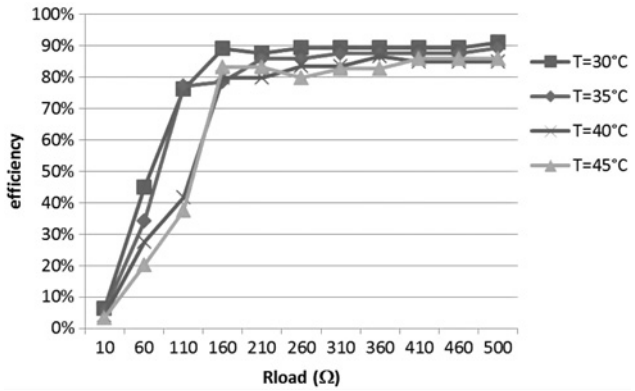

Fig. 9 *Measured system efficiency for different temperatures of the PV cell ($G \simeq 1000$ W/m^2)*

doi: 10.1049/iet-pel.2012.0553

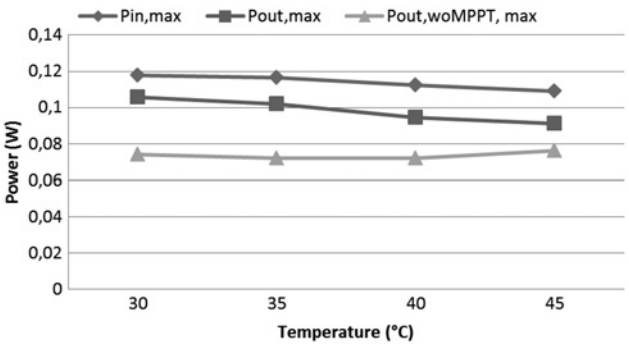

Fig. 10 *Maximum power extraction comparison for different temperatures of the PV cell ($G \simeq 1000\ W/m^2$)*

Fig. 10, reports the measured maximum power levels at the input and output of the circuit, with and without the MPP control loop, for different values of temperature. It can be noted that an 86% average system efficiency over temperature is found when the MPP control loop is active, whereas the average efficiency is 65% when the control loop is deactivated. Therefore a roughly 25% power extraction increment is measured thanks to the MPP circuit.

The results are in good agreement with simulations and confirm the effectiveness of the proposed approach.

5 Conclusion

In this paper, a DC–DC converter with embedded MPPT system for PV micro-scale energy harvesting applications has been presented and confirms the effectiveness of inductorless DC–DC converters (charge pumps) in the power management of micro-scale systems. The proposed solution relies on a straightforward control algorithm which exploits an NTC thermistor to accurately track the MPP voltage against temperature variations. A prototype was implemented using commercial off-the-shelf components and shows an efficiency better than 83% for output powers above 90 mW. The converter is able to extract the maximum power from a PV generator whose MPP voltage ranges from 1.8 to 2.75 V, providing a maximum output power of 330 mW. Further optimisation, especially regarding the efficiency under low current and voltage input levels and reduction of standby power consumption, can be achieved by a full custom integrated-circuit implementation. Presently, the authors are working towards this direction and results will be available in the near future.

6 Acknowledgments

This work is partially supported by the UE (ENIAC Joint Undertaking) in the 'END' project (ENIAC - 120214), and by the Project PON02_00355_3391233 'ENERGETIC' funded by the MIUR (Italian Ministry of Education, University and Scientific Research).

7 References

1 Grasso, A.D., Sapuppo, C., Tina, G.M., Giusto, R.: 'MPPT charge regulator for photovoltaic stand-alone dual battery systems', *Electr. Eng. Res. Report*, 2009, **2**, (1), pp. 1–8
2 Barca, G., Moschetto, A., Sapuppo, C., Tina, G.M., Giusto, R., Grasso, A.D.: 'Optimal energy management of a photovoltaic stand-alone dual battery system'. Proc. MELECON'08, Ajaccio, France, May 2008, pp. 619–624
3 Tina, G.M., Ventura, C., Arena, P., Patanè, L., Grasso, A.D.: 'A novel MPPT charge regulator for a photovoltaic mobile robot application'. Proc. Electrimacs 2011, Cergy-Pontoise, France, June 2011
4 Dondi, D., Bertacchini, A., Brunelli, D., Larcher, L., Benini, L.: 'Modeling and optimization of a solar energy harvester system for self-powered wireless sensor networks', *IEEE Trans. Ind. Electron.*, 2008, **55**, (7), pp. 2759–2766
5 Brunelli, D., Moser, C., Thiele, L., Benini, L.: 'Design of a solar-harvesting circuit for batteryless embedded systems', *IEEE Trans. Circuits Syst. I, Regul. Pap.*, 2009, **56**, (11), pp. 2519–2528
6 Chao, L., Raghunathan, V., Roy, K.: 'Maximum power point considerations in micro-scale solar energy harvesting systems'. Proc. ISCAS 2010, June 2010, pp. 273–276
7 Chini, A., Soci, F.: 'Boost-converter-based solar harvester for low power applications', *Electron. Lett.*, 2010, **46**, (4), pp. 296–298
8 Shao, H., Tsui, C.Y., Ki, W.H.: 'The design of a micro power management system for applications using photovoltaic cells with the maximum output power control', *IEEE Trans. VLSI*, 2009, **17**, pp. 1138–1142
9 Raghunathan, V., Kansal, A., Hsu, J., Friedman, J., Srivastava, M.: 'Design considerations for solar energy harvesting wireless embedded systems', *Proc. IPSN 2005*, 2005, **1**, pp. 457–462
10 Shih, Y.C., Otis, B.P.: 'An inductor-less DC–DC converter for energy harvesting with a 1.2-μW bandgap-referenced output controller' *IEEE Trans. Circuits Syst. II*, 2011, **58**, (12), pp. 832–836
11 Kim, J., Kim, C.: 'A regulated charge pump with a low-power integrated optimum power point tracking algorithm for indoor solar energy harvesting', *IEEE Trans. Circuits Syst. II*, 2011, **58**, (12), pp. 802–806
12 'Power tracking 2A battery charger for solar power', Technical report, datasheet no. LT 0510 REV C, Linear Technol. Corp., Milpitas, CA, 2010
13 Lopez-Lapena, O., Penella, M.T., Gasulla, M.: 'A new MPPT method for low-power solar energy harvesting', *IEEE Trans. Ind. Electron.*, 2010, **57**, pp. 3129–3138
14 Faranda, R., Leva, S., Maugeri, V.: 'MPPT techniques for PV systems: energetic and cost comparison'. Proc. PES 2008, July 2008, pp. 1–6
15 Esram, E., Chapman, P.L.: 'Comparison of photovoltaic array maximum power point tracking techniques', *IEEE Trans. Energy Convers.*, 2007, **22**, (2), pp. 439–449
16 Tse, K.K., Ho, B.M.T., Chung, H.S.-H., Ron Hui, S.Y.: 'A comparative study of maximum-power-point trackers for photovoltaic panels using switching-frequency modulation scheme', *IEEE Trans. Ind. Electron.*, 2004, **51**, (2), pp. 410–418
17 Gao, L., Dougal, R.A., Liu, S., Iotova, A.P.: 'Parallel-connected solar PV system to address partial and rapidly fluctuating shadow conditions', *IEEE Trans. Ind. Electron.*, 2009, **56**, (5), pp. 1548–1556
18 Pulvirenti, F., La Scala, A., Ragonese, D., D'Souza, K., Tina, G.M., Pennisi, S.: '4-phase interleaved boost converter with IC controller for distributed photovoltaic systems', IEEE Trans. Circuits Syst. I, in print
19 Seeman, M., Ng, V., Le, H.-P., John, M., Alon, E., Sanders, S.: 'A comparative analysis of switched-capacitor and inductor-based dc-dc conversion technologies'. IEEE Workshop on Control and Modelling for Power Electronics (COMPEL 2010), June 2010, pp. 1–7
20 Seeman, M., Sanders, S.: 'Analysis and optimization of switched-capacitor DC–DC converters', *IEEE Trans. Power Electron.*, 2008, **23**, (2), pp. 841–851
21 Palumbo, G., Pappalardo, D.: 'Charge pump circuits: power consumption optimization', *IEEE Trans. Circuits Syst.*, 2002, **49**, (11), pp. 1535–1542
22 Chowdhury, I., Dongsheng, M.: 'Design of reconfigurable and robust integrated SC power converter for self-powered energy-efficient devices', *IEEE Trans. Ind. Electron.*, 2009, **56**, (10), pp. 4018–4028
23 Yong, F., Zhenfei, P., Shanshan, Y., Zhiliang, H., Yang, L.: 'A dual mode charge pump with adaptive output used in a class G audio power amplifier', *J. Semiconductors*, 2011, **32**, (4), pp. 045002-1–045002-9
24 Le, H.-P., Seeman, M., Sanders, S., Sathe, V., Naffziger, S., Alon, E.: 'A 32 nm fully integrated reconfigurable switched-capacitor DC–DC converter delivering 0.55 W/mm^2 at 81% Efficiency', ISSCC Dig. Technical Papers, 2010, pp. 210–211
25 'LTC3221 micropower regulated charge pump in 2 × 2 DFN', Technical report, datasheet no. LT 1006, Linear Technol. Corp., Milpitas, CA, 2006
26 'LTC1540 Nanopower comparator with reference', Technical report, datasheet no. LT 0403 REV A, Linear Technol. Corp., Milpitas, CA, 1997